

St. John Fisher College

## Fisher Digital Publications

---

Biology Faculty/Staff Publications

Biology

---

5-2012

### Drag Reduction in Wave-Swept Macroalgae: Alternative Strategies and New Predictions

Patrick T. Martone

Laurie Kost

Michael L. Boller

Saint John Fisher College, mboller@sjfc.edu

Follow this and additional works at: [https://fisherpub.sjfc.edu/biology\\_facpub](https://fisherpub.sjfc.edu/biology_facpub)



Part of the [Biology Commons](#)

### [How has open access to Fisher Digital Publications benefited you?](#)

---

#### Publication Information

Martone, Patrick T.; Kost, Laurie; and Boller, Michael L. (2012). "Drag Reduction in Wave-Swept Macroalgae: Alternative Strategies and New Predictions." *American Journal of Botany* 99.5, 806-815. Please note that the Publication Information provides general citation information and may not be appropriate for your discipline. To receive help in creating a citation based on your discipline, please visit <http://libguides.sjfc.edu/citations>.

This document is posted at [https://fisherpub.sjfc.edu/biology\\_facpub/4](https://fisherpub.sjfc.edu/biology_facpub/4) and is brought to you for free and open access by Fisher Digital Publications at St. John Fisher College. For more information, please contact [fisherpub@sjfc.edu](mailto:fisherpub@sjfc.edu).

---

# Drag Reduction in Wave-Swept Macroalgae: Alternative Strategies and New Predictions

## Abstract

Premise of the study: Intertidal macroalgae must resist extreme hydrodynamic forces imposed by crashing waves. How does frond flexibility mitigate drag, and how does flexibility affect predictions of drag and dislodgement in the field? Methods: We characterized flexible reconfiguration of six seaweed species in a recirculating water flume, documenting both shape change and area reduction as fronds reorient. We then used a high-speed gravity-accelerated water flume to test our ability to predict drag under waves based on extrapolations of drag recorded at slower speeds. We compared dislodgement forces to drag forces predicted from slow- and high-speed data to generate new predictions of survivorship and maximum sustainable frond size along wave-swept shores. Key results: Bladed algae were generally "shape changers", limiting drag by reducing drag coefficients, whereas the branched alga *Calliarthron* was an "area reducer", limiting drag by reducing projected area in flow. Drag predictions often underestimated actual drag measurements at high speeds, suggesting that slow- speed data may not reflect the performance of flexible seaweeds under breaking waves. Several seaweeds were predicted to dislodge at similar combinations of velocity and frond size, suggesting common scaling factors of dislodgement strength and drag. Conclusions: Changing shape and reducing projected area in flow are two distinct strategies employed by flexible seaweeds to resist drag. Flexible reconfiguration contributes to the uncertainty of drag extrapolation, and researchers should use caution when predicting drag and dislodgement of seaweeds in the field.

## Keywords

algae, biomechanics, dislodgement, drag coefficient (C-d), evolution, intertidal, macrophyte, morphology, reconfiguration, seaweed

## Disciplines

Biology

## DRAG REDUCTION IN WAVE-SWEPT MACROALGAE: ALTERNATIVE STRATEGIES AND NEW PREDICTIONS<sup>1</sup>

PATRICK T. MARTONE<sup>2,5</sup>, LAURIE KOST<sup>3</sup>, AND MICHAEL BOLLER<sup>4</sup>

<sup>2</sup>Department of Botany and Biodiversity Research Centre, University of British Columbia, Vancouver, British Columbia V6T 1Z4 Canada; <sup>3</sup>Hopkins Marine Station of Stanford University, Pacific Grove, California 93950 USA; <sup>4</sup>St. John Fisher College, Rochester, New York 14618 USA

- *Premise of the study:* Intertidal macroalgae must resist extreme hydrodynamic forces imposed by crashing waves. How does frond flexibility mitigate drag, and how does flexibility affect predictions of drag and dislodgement in the field?
- *Methods:* We characterized flexible reconfiguration of six seaweed species in a recirculating water flume, documenting both shape change and area reduction as fronds reorient. We then used a high-speed gravity-accelerated water flume to test our ability to predict drag under waves based on extrapolations of drag recorded at slower speeds. We compared dislodgement forces to drag forces predicted from slow- and high-speed data to generate new predictions of survivorship and maximum sustainable frond size along wave-swept shores.
- *Key results:* Bladed algae were generally “shape changers”, limiting drag by reducing drag coefficients, whereas the branched alga *Calliarthron* was an “area reducer”, limiting drag by reducing projected area in flow. Drag predictions often underestimated actual drag measurements at high speeds, suggesting that slow-speed data may not reflect the performance of flexible seaweeds under breaking waves. Several seaweeds were predicted to dislodge at similar combinations of velocity and frond size, suggesting common scaling factors of dislodgement strength and drag.
- *Conclusions:* Changing shape and reducing projected area in flow are two distinct strategies employed by flexible seaweeds to resist drag. Flexible reconfiguration contributes to the uncertainty of drag extrapolation, and researchers should use caution when predicting drag and dislodgement of seaweeds in the field.

**Key words:** algae; biomechanics; dislodgement; drag coefficient ( $C_d$ ); evolution; intertidal; macrophyte; morphology; reconfiguration; seaweed.

Waves crashing on shore impose extraordinary hydrodynamic forces on intertidal organisms (Denny, 1988, 1994; Denny et al., 2003). Wave-induced forces affect the survivorship, distribution, and interactions of intertidal animals and algae, thereby influencing population dynamics (Paine, 1979; Blanchette, 1996), zonation patterns (Lewis, 1968; Harley and Helmuth, 2003; Harley and Paine, 2009), and community structure (Connell, 1972; Denny and Wethey, 2001), and making the intertidal zone an excellent test bed for evolutionary and ecological studies (e.g., Dayton, 1975; Sousa, 1979; Paine and Levin, 1981; Harley, 2003; Stachowicz et al., 2008). For example, seaweeds clinging to intertidal rocks must resist wave-induced hydrodynamic forces to survive, just as some terrestrial plants must resist strong winds (Vogel, 1989; Ennos, 1997, 1999; Niklas and Speck, 2001; Butler et al., 2012). Seaweeds that are broken, dislodged, and cast ashore after big storms are testaments to the selective pressures applied by breaking waves. Because seaweeds are foundational species that comprise both food and habitat for animals along the shore, loss of seaweed populations due to wave-induced forces can have cascading effects on intertidal

marine communities. Thus, understanding biomechanical adaptations of seaweeds to reduce or resist hydrodynamic forces will help us predict patterns of dislodgement and shifts in near-shore ecology and potentially provide insight into aerodynamic influences on terrestrial plants (Denny, 1994; Ennos, 1999).

Biomechanists have applied engineering principles to quantify hydrodynamic forces experienced by intertidal seaweeds to resolve differences across morphologies and to predict patterns of dislodgement along the shore (Koehl, 1986; Carrington, 1990; Gaylord et al., 1994; Gaylord and Denny, 1997; Hurd, 2000; Denny and Gaylord, 2002; Boller and Carrington, 2006b, 2007; Mach et al., 2011). Among fluid forces, drag has received the most attention, although forces resulting from wave impingement and seaweed inertia have also been demonstrated (Gaylord, 2000; Gaylord et al., 2008). According to previous studies, seaweeds of widely varying morphology often perform similarly in flow because they are flexible. Unlike rigid engineering shapes, such as cones and cylinders, flexible seaweeds “reconfigure” in flow: blades curl up and branches collapse and fold together as water velocity increases, thereby reducing the surface area of fronds projected into the flow and changing shape to limit drag (Carrington, 1990; Denny and Gaylord, 2002; Harder et al., 2004; Boller and Carrington, 2006b).

Boller and Carrington (2006b, 2007) were the first to distinguish between shape change and area reduction in flow, the two drag-limiting processes associated with flexible reconfiguration. Their data demonstrate that some seaweed morphologies are better at reducing projected area in flow, while others are better at reducing drag coefficient ( $C_d$ , a parameter that varies with shape). This distinction suggests two morphological strategies exist for limiting imposed drag force: the capacity of flexible

<sup>1</sup>Manuscript received 15 November 2011; revision accepted 15 March 2012.

The authors thank M. W. Denny for his insight, encouragement, and financial support. This manuscript benefited from comments contributed by L. Anderson, B. Claman, R. Guenther, and J. Jorve. Funding was provided by the National Science Foundation (IOS-0641068, IOS-1052161) to M. W. Denny and by the Natural Sciences and Engineering Research Council to P. T. Martone.

<sup>5</sup>Author for correspondence: (e-mail: pmartone@mail.ubc.ca)

thalli to change shape or to reduce size. If selection can act on either shape or size changes, then two flexible seaweeds of widely divergent sizes or shapes may ultimately experience similar drag under crashing waves. For example, bladed and branched seaweeds often coexist along the shore, suggesting that either form is sufficient to resist drag. Furthermore, seaweeds that are morphologically similar but phylogenetically distant, such as bladed algae in the Rhodophyte genus *Porphyra*, the Chlorophyte genus *Ulva*, and the Phaeophyceyan genus *Petalonia*, likely reflect parallel evolution of morphology perhaps canalized in response to selective pressures related to wave-induced drag. Exploring the dynamics of size and shape change of intertidal seaweeds in flow may reveal potential strategies underlying morphological divergence and canalization and may help us understand the evolutionary pressures that gave rise to the diversity of macroalgae along wave-swept rocky shores.

Flexible reconfiguration complicates predictions of drag and dislodgement in the field, as seaweeds flop, twist, and reconfigure in flow. Drag measurements recorded in the laboratory in recirculating flumes ( $<5 \text{ m}\cdot\text{s}^{-1}$ ) must be extrapolated to environmentally relevant water velocities (up to  $25 \text{ m}\cdot\text{s}^{-1}$ ) (Denny and Gaylord, 2002; Denny et al., 2003; Helmuth and Denny, 2003). This extrapolation process is fraught with potential error largely because of uncertainty in reconfiguration ( $C_d$ ) at high speeds (Vogel, 1994; Bell, 1999). Past studies have reported wide discrepancies between drag predictions made in the laboratory and observations of dislodgement in the field (Gaylord et al., 1994), although some of this error was likely due to a lack of consideration for fatigue of algal tissues under breaking waves (Mach et al., 2007, 2011; Mach, 2009). One notable exception was a recent study by Martone and Denny (2008) that accurately predicted the maximum size of intertidal seaweeds by characterizing drag and dislodgement in a high-speed gravity-accelerated water flume, which generated flow speeds up to  $10 \text{ m}\cdot\text{s}^{-1}$ . The accuracy of their predictions suggests that high-speed measurements may increase our predictive power by reducing the need for extrapolation. But what speeds are sufficient to make accurate predictions?

In this study, we investigate drag and flexible reconfiguration of six morphologically distinct seaweeds in flow. We characterize size and shape change as water velocity increases to explore morphological strategies to mitigate selective pressures applied by wave-induced drag forces. We measure drag and reconfiguration of seaweeds in a recirculating flume up to  $4 \text{ m}\cdot\text{s}^{-1}$ , and then examine the error involved in extrapolation by testing our drag predictions at  $6.8$  and  $9.5 \text{ m}\cdot\text{s}^{-1}$  in the high-speed water flume described in Martone and Denny (2008). Finally, we generate updated models of drag and dislodgement for each seaweed species based on all drag measurements up to  $9.5 \text{ m}\cdot\text{s}^{-1}$ , and we test these new models by comparing predicted and observed limits to maximum frond sizes in the field.

## MATERIALS AND METHODS

**Specimen collection**—Seaweeds representing a range of branched and bladed morphologies were collected from the intertidal zone at Hopkins Marine Station, Pacific Grove, California. Fronds ( $N = 10$ ) were collected from each of the following species: *Calliarthron cheilosporioides* Manza, *Chondracanthus exasperatus* (Harvey & J.W.Bailey) J.R.Hughey, *Mazzaella flaccida* (Setchell & N.L.Gardner) Fredericq, *Mastocarpus papillatus* (C.Agardh) Kützing, *Prionitis lanceolata* (Harvey) Harvey, and *Codium fragile* (Suringar) Hariot. Seaweeds were examined and epiphytes were removed. Seaweeds were maintained in running seawater for less than 2 d before experimentation.

**Quantifying reconfiguration**—Seaweeds were affixed to a calibrated 2-axis force transducer (US-6002, Bokam Engineering, Santa Ana, California, USA) using cyanoacrylate glue. The force transducer was then secured into a recirculating water flume with the seaweed standing erect, perpendicular to the direction of flow. Drag was measured on each seaweed at the following 15 velocities: 0, 0.1, 0.2, 0.3, 0.5, 0.8, 1.2, 1.5, 1.9, 2.3, 2.7, 3.1, 3.4, and  $4.0 \text{ m}\cdot\text{s}^{-1}$ . Free stream velocities were calibrated using an acoustic Doppler velocimeter (ADV Vectrino, Nortek, Rud, Norway). At each velocity, reconfiguring seaweeds were photographed (EOS 30D, Canon) from downstream (see Fig. 1), and seaweed projected areas ( $A_{\text{proj}}$ ) were calculated from the average area measured from three photographs using the program ImageJ (National Institutes of Health, Washington, D.C., USA). After each trial, seaweeds were spread out flat and photographed from above to measure maximum area ( $A_{\text{max}}$ , equivalent to half the wetted surface area).

True drag coefficient ( $C_{d, \text{true}}$ ) was calculated at each velocity according to the following equation:

$$C_{d, \text{true}} = \frac{2 F_{\text{drag}}}{\rho U^2 A_{\text{proj}}}, \quad (1)$$

where  $F_{\text{drag}}$  is drag force (N),  $\rho$  is density of water ( $1000 \text{ kg}\cdot\text{m}^{-3}$ ),  $U$  is water velocity ( $\text{m}\cdot\text{s}^{-1}$ ), and  $A_{\text{proj}}$  is seaweed projected area ( $\text{m}^2$ ) measured from downstream as described above. Differences in true drag coefficients at  $4 \text{ m}\cdot\text{s}^{-1}$  were detected using a nested two-way ANOVA with factors morphology (2 levels: bladed and branched) and species (6 levels, nested within morphology). Species differences were compared using Tukey's honestly significant difference (HSD) posthoc.

Normalized area ( $A_{\%}$ ) was calculated at each velocity according to the following equation:

$$A_{\%} = \frac{A_{\text{proj}}}{A_{\text{max}}} \times 100. \quad (2)$$

Differences in normalized areas at  $4 \text{ m}\cdot\text{s}^{-1}$  were detected using a nested two-way ANOVA with factors morphology and species, as defined above. Species differences were compared using Tukey's honestly significant difference (HSD) posthoc.

True drag coefficient ( $C_{d, \text{true}}$ ) and normalized area ( $A_{\%}$ ) were plotted against water velocity to provide dimensionless indices of changes in seaweed shape and size with increasing velocity. The product of true drag coefficient and normalized area ( $C_{d, \text{true}} \cdot A_{\%}$ ) was plotted against water velocity to examine total reconfiguration, the combined effect of both size change and shape change with increasing velocity. Differences in total reconfiguration ( $C_{d, \text{true}} \cdot A_{\%}$ ) at  $4 \text{ m}\cdot\text{s}^{-1}$  were detected using a nested two-way ANOVA with factors morphology and species, as defined above. Species differences were compared using Tukey's HSD post hoc test.

**Predicting drag at higher velocities**—To facilitate extrapolations of drag, we combined the effect of water velocity and frond size into frond Reynolds number ( $Re_f$ ):

$$Re_f = \frac{UL}{\nu} = \frac{U\sqrt{A_{\text{max}}}}{\nu}, \quad (3)$$

where  $\nu$  is the kinematic viscosity of water ( $1 \times 10^{-6} \text{ m}^2\cdot\text{s}^{-1}$ ) and  $L$  is the characteristic length (m). This  $Re_f$  method was first applied successfully by Martone and Denny (2008). New drag coefficients ( $C_{d, \text{planform}}$ ), based on maximum frond area, were calculated for each seaweed at frond Reynolds numbers tested in the recirculating water flume.

$$C_{d, \text{planform}} = \frac{2F_{\text{drag}}}{\rho U^2 A_{\text{max}}} = \frac{2F_{\text{drag}}}{\rho(\nu Re_f)^2}. \quad (4)$$

For each species,  $C_{d, \text{planform}}$  was plotted against  $Re_f$ , and power curves were fitted to log-transformed data using the program Matlab (v7.0.1, The Mathworks, Natick, Massachusetts, USA), and 95% confidence intervals (CI) around the fitted curves were calculated from 1000 bootstrapped data sets each composed of 10 data points haphazardly sampled from the original data and each data point representing a unique plant and velocity to ensure independence (Efron and Tibshirani, 1993). Estimates of  $C_{d, \text{planform}}$  (mean  $\pm 95\%$  CI) were then used to estimate drag force up to  $\log Re_f = 6.5$ , according to the following equation:

$$\begin{aligned} F_{\text{drag}} &= \frac{1}{2} \rho U^2 A_{\text{max}} C_{d, \text{planform}} \\ &= \frac{1}{2} \rho (\nu Re_f)^2 C_{d, \text{planform}}. \end{aligned} \quad (5)$$

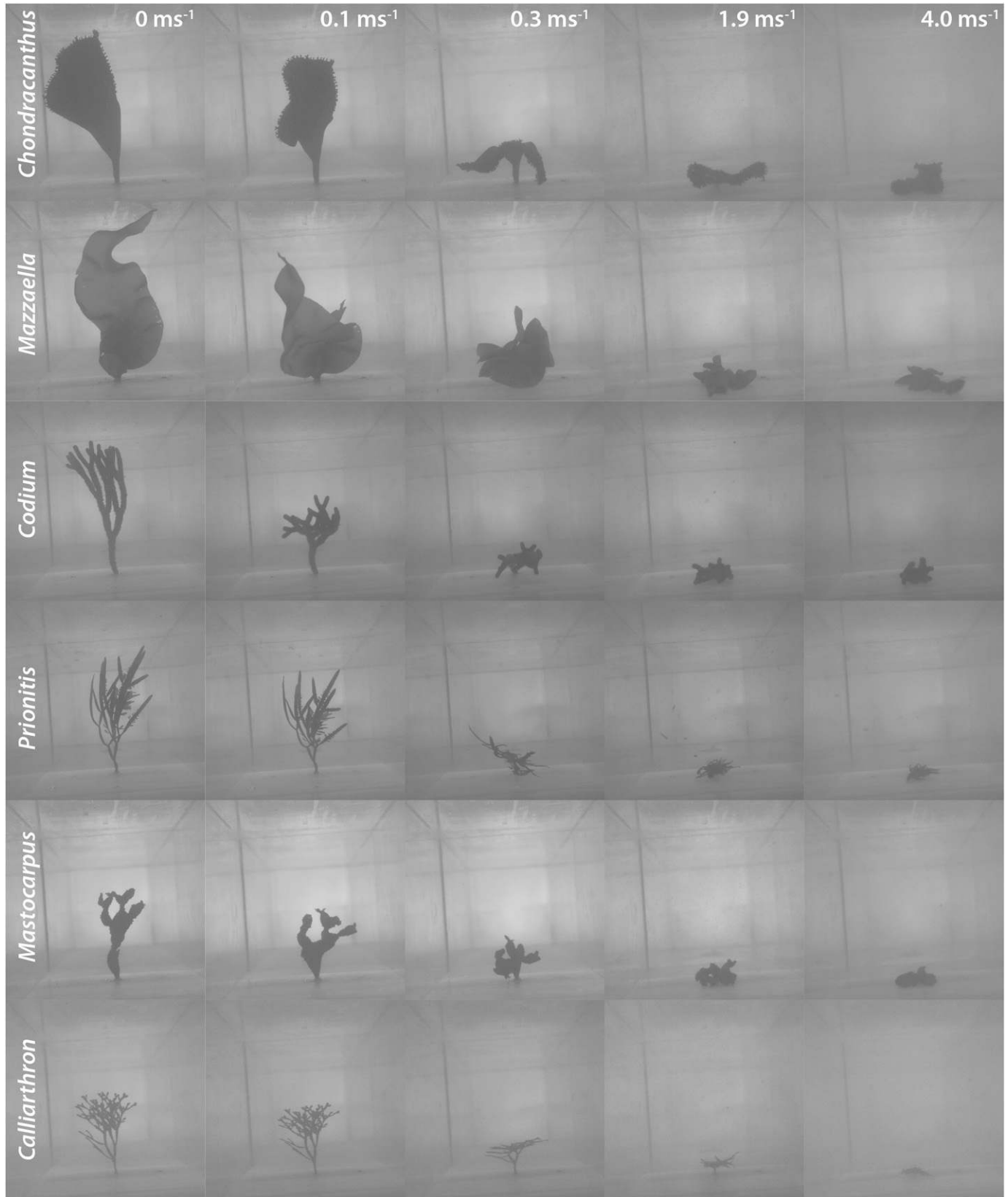


Fig. 1. Seaweeds reconfiguring in flow, viewed from downstream.



To test these drag predictions, we collected additional fronds: *Calliarthron cheilosporioides* ( $N = 10$ ), *Chondracanthus exasperatus* ( $N = 10$ ), *Mazzaella flaccida* ( $N = 10$ ), *Mastocarpus papillatus* ( $N = 10$ ), *Prionitis lanceolata* ( $N = 12$ ), and *Codium fragile* ( $N = 11$ ). Maximum planform areas ( $A_{\max}$ ) of fronds were measured and recorded as described above. Seaweeds were affixed to a custom force transducer using cyanoacrylate glue and then secured into a gravity-accelerated water flume (illustrated in fig. 3 in Martone and Denny, 2008). Drag was measured on each frond in bursts of water moving 6.8 and 9.5  $\text{m}\cdot\text{s}^{-1}$ , simulating waves crashing onshore. Drag measurements were plotted against frond Reynolds numbers ( $Re_f$ , calculated from Eq. 3) and visually compared to predictions based on data generated in the recirculating flume.

**New predictions of size and survival**—For each species, drag measurements collected in the recirculating and gravity-accelerated flumes were combined into a single data set, and new curves were fitted to log-transformed  $C_{d, \text{planform}}$  vs.  $Re_f$  data. Data collected in the gravity flume were weighted to equalize the number of datapoints analyzed from each flume and to ensure that predictive curves were mostly based on high-speed data. Estimates of  $C_{d, \text{planform}}$  were used to estimate drag force up to  $log Re_f = 6.5$ , according to Eq. 5.

Dislodgement forces were recorded for each seaweed species in the field at Hopkins Marine Station. Fronds ( $N = 20$ ) from *Prionitis*, *Chondracanthus*, *Codium*, and *Mazzaella* were pulled from the rock by attaching a clip near the base of the fronds and using a 5000-g spring scale to record dislodgement force parallel to the substratum. Dislodgement forces of *Calliarthron* were reported by Martone (2006), and dislodgement forces of *Mastocarpus* were reported by Kitzes and Denny (2005). Maximum dislodgement forces were noted, and maximum percentiles were calculated assuming normal distributions and using mean and standard deviation values for each species (Sokal and Rohlf, 2001).

Fronds were predicted to break when drag force and dislodgement force were equal, and maximum dislodgement force represented the maximum drag force that fronds could resist. For each species, drag force was set equal to maximum dislodgement force to calculate the critical frond Reynolds number ( $Re_{f, \text{crit}}$ ), the combination of frond size and water velocity that would dislodge all fronds. This was done by iteratively solving Eq. 5 for values of  $Re_f$  until dislodgement force was reached.  $Re_{f, \text{crit}}$  was then used to calculate water velocities that would dislodge fronds of a given size or, conversely, the maximum size to which fronds could grow without being dislodged at a given velocity (see Eq. 6). Field observations were used to test these predictions.

$$A_{\text{crit}} = \left( \frac{v Re_{f, \text{crit}}}{U_{\text{crit}}} \right)^2 \quad (6)$$

## RESULTS

**Quantifying reconfiguration**—As water velocity increased in the recirculating flume, fronds reconfigured (Fig. 1), and true drag coefficient decreased for all seaweed species (Fig. 2A). Branched algae *Calliarthron* and *Mastocarpus* had the highest  $C_{d, \text{true}}$  at all test velocities (Fig. 2A). At 4  $\text{m}\cdot\text{s}^{-1}$ ,  $C_{d, \text{true}}$  values for bladed algae were significantly lower than  $C_{d, \text{true}}$  for branched algae ( $F_{1, 45} = 150.30$ ,  $P < 0.001$ , Table 1). On average, *Calliarthron* had the highest  $C_{d, \text{true}}$  at 4  $\text{m}\cdot\text{s}^{-1}$  ( $0.54 \pm 0.04$ ), whereas *Mazzaella* had the lowest  $C_{d, \text{true}}$  ( $0.08 \pm 0.02$ ) ( $F_{4, 45} = 15.16$ ,  $P < 0.001$ , Tukey's HSD results in Table 1).

As water velocity increased, normalized area also decreased for all seaweed species (Figs. 1, 2B). Normalized area of *Calliarthron* fronds decreased more than that of other seaweeds. At 4  $\text{m}\cdot\text{s}^{-1}$ , normalized area of *Calliarthron* decreased to  $6.2 \pm 0.5\%$  of maximum frond area, more area reduction than all other seaweeds investigated ( $F_{4, 45} = 24.29$ ,  $P < 0.001$ , Tukey's HSD results in Table 1). At 4  $\text{m}\cdot\text{s}^{-1}$ , normalized areas of other seaweeds decreased to 14.9–22.9%, on average, and did not differ significantly by morphology ( $F_{1, 45} = 1.30$ ,  $P = 0.26$ ) or by species (Tukey's HSD results in Table 1).

The combination of true drag coefficient and normalized area also decreased with increasing water velocity (Fig. 2c). In general, bladed algae reconfigured significantly more than

branched algae ( $F_{1, 45} = 68.53$ ,  $P < 0.001$ ). *Mazzaella* reconfigured significantly more than all other seaweeds ( $F_{4, 45} = 10.87$ ,  $P < 0.001$ , Tukey's HSD results in Table 1). Considering both shape and area change, reconfiguration of *Calliarthron* fronds was comparable to other seaweeds (Fig. 2C, Tukey's HSD results in Table 1).

**Predicting drag at higher velocities**—Experiments in the recirculating water flume generated drag data in the range of  $log Re_f$  from approximately 3.5–5.5 (Fig. 3). For all species, recalculated drag coefficients ( $C_{d, \text{planform}}$ ) decreased as  $Re_f$  increased (Fig. 3). Curves fitted to  $C_{d, \text{planform}}$  vs.  $Re_f$  data generally had little margin of error (Fig. 3); however, extrapolations of drag force beyond the data often had wide margins of error and were not always accurate (Fig. 4). For *Codium*, *Prionitis*, *Mastocarpus*, and *Chondracanthus*, data collected in the recirculating water flume were reasonably successful in predicting drag at higher  $Re_f$  (Fig. 4B–E). However, for *Calliarthron* and *Mazzaella*, data collected in the recirculating flume often under-predicted drag experienced by fronds at higher  $Re_f$  (Fig. 4A, F). Predictions for *Mazzaella* were particularly poor; drag forces on *Mazzaella* fronds were many times higher than those predicted (Fig. 4F).

**Predicting dislodgement**—With increasing  $Re_f$ , drag on *Codium* and *Mastocarpus* was predicted to increase similarly and at a faster rate than drag on other seaweeds (Fig. 5A). Drag on *Chondracanthus* and *Prionitis* was also predicted to increase similarly (Fig. 5A). Among the seaweeds studied, drag on *Mazzaella* blades was predicted to increase most slowly with increasing  $Re_f$  (Fig. 5A).

Maximum dislodgement forces of the six seaweed species are listed in Table 2. Maximum forces ranked above the 89th percentile of dislodgement forces for each species (Table 2), suggesting that these forces would be sufficient to dislodge at least 89% of the individuals of each species. Maximum dislodgement forces were used in conjunction with drag prediction curves to calculate  $Re_{f, \text{crit}}$  values (Table 2, Fig. 5A).  $Re_{f, \text{crit}}$  values were similar (approximately  $2 \times 10^6$ ) for four wave-exposed species: *Prionitis*, *Calliarthron*, *Chondracanthus*, and *Mazzaella* (Table 2, Fig. 5A).  $Re_{f, \text{crit}}$  values of *Codium* ( $0.989 \times 10^6$ ) and *Mastocarpus* ( $0.479 \times 10^6$ ) were lower than those of the other four species.  $Re_{f, \text{crit}}$  values generated isoclines for each species depicting decreasing maximum frond size with increasing velocity (Fig. 5B). Larger fronds were predicted to break at slower velocities; smaller fronds were predicted to break at faster velocities (Fig. 5B). Isoclines for *Prionitis*, *Calliarthron*, *Chondracanthus*, and *Mazzaella* were similar, and for any water velocity these four species were predicted to support larger fronds than *Codium* or *Mastocarpus* (Fig. 5B). The maximum observed size of *Mazzaella* and *Chondracanthus* were similar and were predicted to resist similar water velocities (Fig. 5B). The maximum observed size of *Mastocarpus* and *Calliarthron* were similar (approximately 40  $\text{cm}^2$ ), but at this size *Calliarthron* was predicted to resist nearly four times the water velocity before breaking (Fig. 5B).

## DISCUSSION

**Hydrodynamic selective pressures**—During reconfiguration, shape change and area reduction occur concurrently, yet they are somewhat independent of one another: seaweeds that quickly reduce projected areas may maintain relatively high

drag coefficients, and seaweeds that are exceptionally good at reducing drag coefficients may maintain large projected areas. In other words, seaweeds specializing in area reduction or shape change may experience similar drag despite morphological differences. Thus, as seaweeds have evolved in hydrodynamically stressful habitats like the wave-swept intertidal zone, selection may have acted on the ability of macroalgal thalli to either change shape or to reduce area in flow.

Our data illustrate these two strategies for drag limitation. For example, drag coefficients of the articulated coralline *Calliarthron* are consistently higher than drag coefficients of all other algae in this study, suggesting that its calcified, segmented structure is particularly drag prone. However, *Calliarthron* fronds compensate for high drag coefficients by being exceptionally good at reducing projected area as flow rates increase. When both shape change and area reduction are taken into account, total reconfiguration of *Calliarthron* fronds is intermediate

and not unlike other seaweeds (Fig. 2C). Thus, *Calliarthron* is an “area reducer,” limiting drag primarily by reducing frond area projected into flow, not by changing shape.

Bladed algae, on the other hand, are “shape changers.” Both *Chondracanthus* and *Mazzaella* have significantly lower drag coefficients than branched algae at the highest experimental velocities (Fig. 2A). However, their capacity to reduce projected area in flow was comparable to other branched algae. When shape change and area reduction are taken into account, *Chondracanthus* and *Mazzaella* reconfigured more than most seaweeds, and *Mazzaella* significantly so. As “shape changers,” *Mazzaella* and *Chondracanthus* limit drag primarily by reducing drag coefficient, not necessarily by reducing projected area. The slight advantage of blades to limit drag may help explain how many of the largest seaweeds, such as *Durvillaea* spp., *Saccharina* spp., and *Pleurophyucus* sp., are able to support this morphology in hydrodynamically stressful habitats.

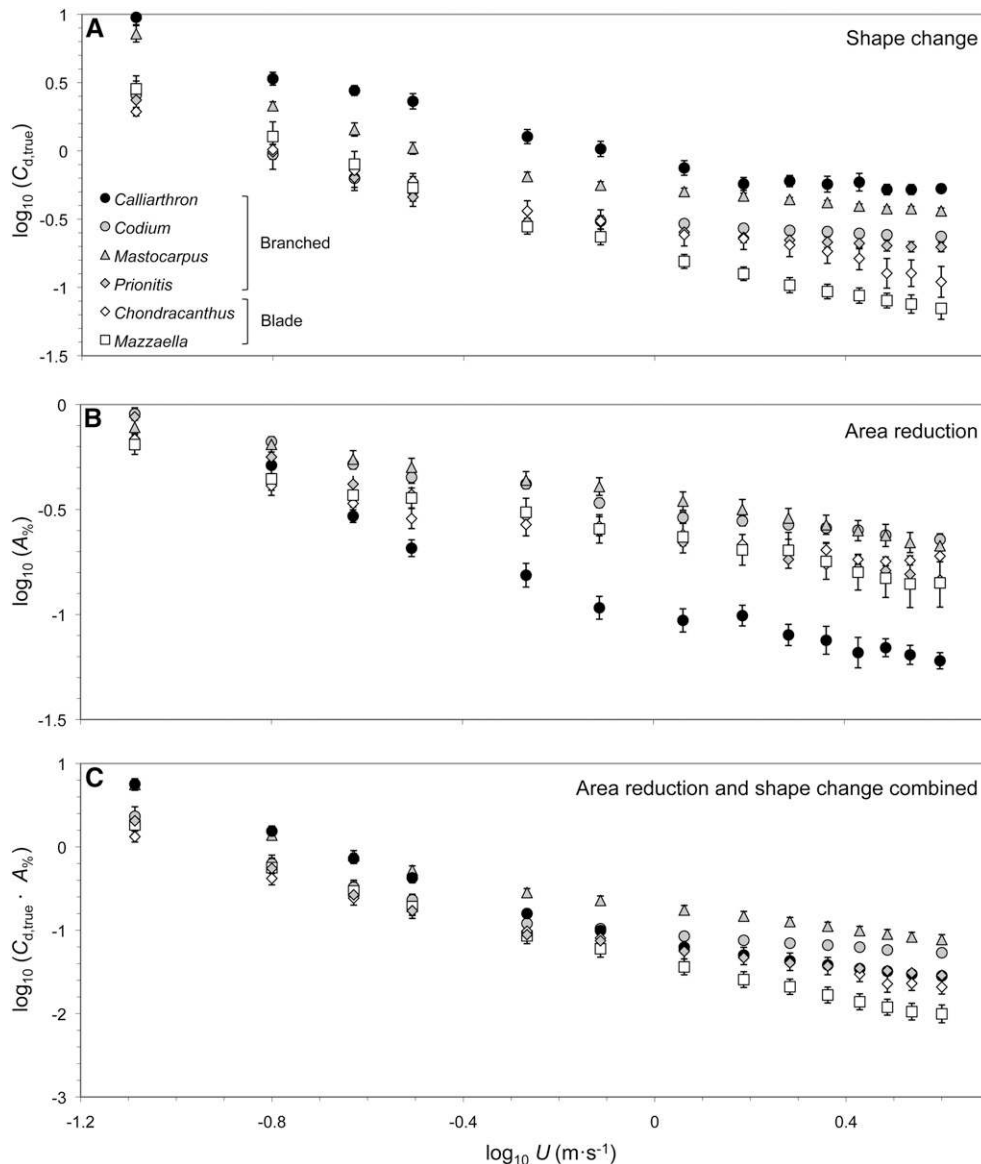


Fig. 2. Quantifying shape change and area reduction of seaweed thalli with increasing water velocity. (A) Reduction in true drag coefficient ( $C_{d,true}$ ). (B) Reduction of projected area ( $A\%$ ). (C) Combined reduction of true drag coefficient and projected area ( $C_{d,true} \cdot A\%$ ).

TABLE 1. Drag coefficients and projected areas of each species at 4 m·s<sup>-1</sup>.

Species	$C_{d,true}$	$A_{\%}$	$C_{d,true} \cdot A_{\%}$	Morphology
<i>Calliarthron</i>	0.54 ± 0.04 a	6.2 ± 0.5 a	0.033 ± 0.002 bc	branched
<i>Codium</i>	0.24 ± 0.01 b	22.9 ± 0.9 bc	0.054 ± 0.004 ab	branched
<i>Mastocarpus</i>	0.37 ± 0.02 a	22.8 ± 3.1 bcd	0.085 ± 0.043 a	branched
<i>Prionitis</i>	0.20 ± 0.02 b	14.9 ± 1.1 bd	0.029 ± 0.005 c	branched
<i>Chondracanthus</i>	0.13 ± 0.03 c	19.2 ± 1.2 bcd	0.024 ± 0.004 c	blade
<i>Mazzaella</i>	0.08 ± 0.02 c	18.8 ± 7.6 bcd	0.013 ± 0.003 d	blade

Notes:  $C_{d,true}$  = true drag coefficient,  $A_{\%}$  = normalized projected area, letters within each column indicate differences among species based on post-hoc Tukey’s tests ( $P < 0.05$ ).

Certainly, these two strategies for drag limitation are not exclusive of one another; some algae likely employ both strategies equally. For example, across all test velocities, the branched alga *Prionitis* exhibits intermediate drag coefficients, intermediate projected areas and, indeed, intermediate levels of total reconfiguration. Thus, *Prionitis* is not clearly an “area reducer” or a “shape changer”. Nevertheless, distinguishing between these two adaptive strategies for reducing drag will help us understand the selective pressures influencing the morphological evolution of wave-swept seaweeds. Unfortunately, both shape change and area reduction are dynamic

processes that are difficult to predict once seaweeds are collected and removed from natural flow conditions. Selection must act on “the ability to change shape” or “the ability to reduce projected area,” and these two abilities are not obviously linked to static algal morphologies. Indeed, under natural flow conditions, seaweeds of differing morphology all start to look similar (see Fig. 1). As past studies have explored the interaction between material properties and drag (Koehl, 1986; Denny et al., 1997; Gaylord and Denny, 1997; Koehl, 2000; Boller and Carrington, 2007; Demes et al., 2011), future studies may find value in material properties, such as Young’s

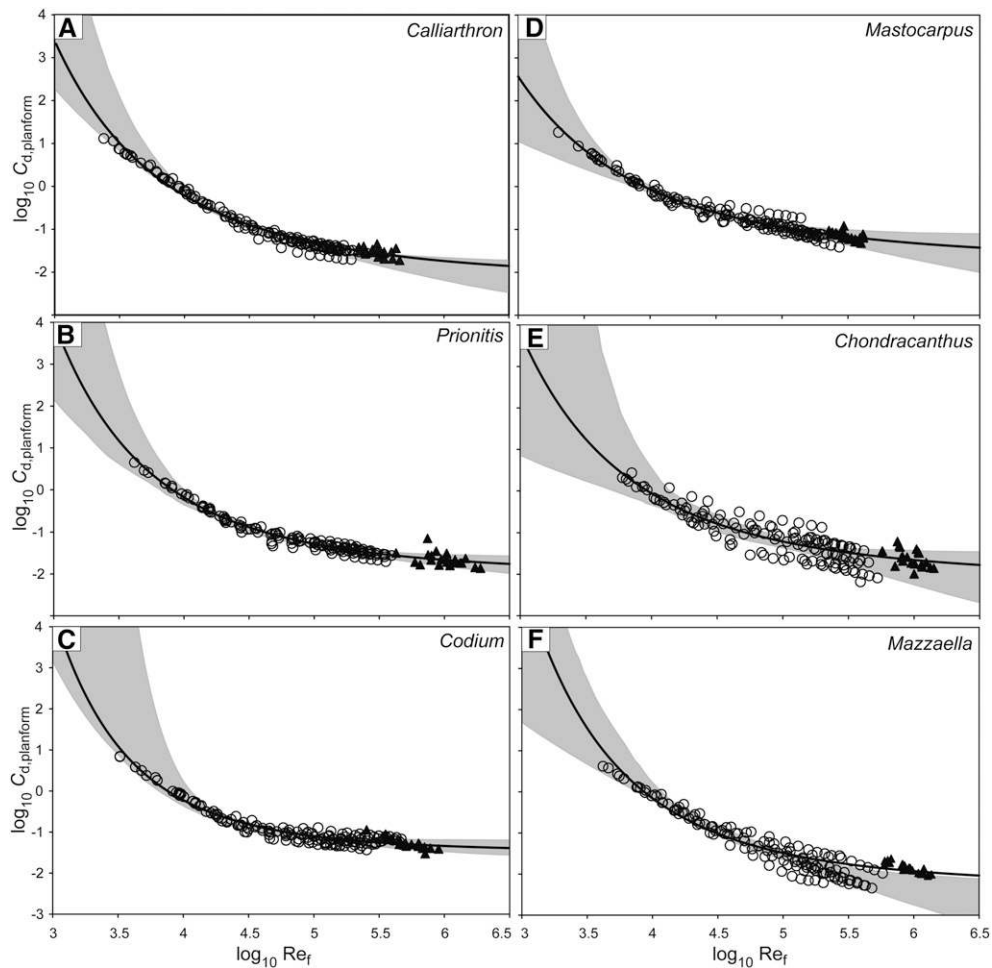


Fig. 3. Drag coefficient ( $C_{d,platform}$ ) vs. front Reynolds number ( $Re_f$ ) for each experimental species. Open circles are data collected in the recirculating flume, and gray regions represent  $\pm 95\%$  confidence intervals around predictions based on flume data alone. Black triangles are data collected in the high-speed gravity flume; solid lines are curves fitted to both recirculating and gravity flume data, as described in the methods.



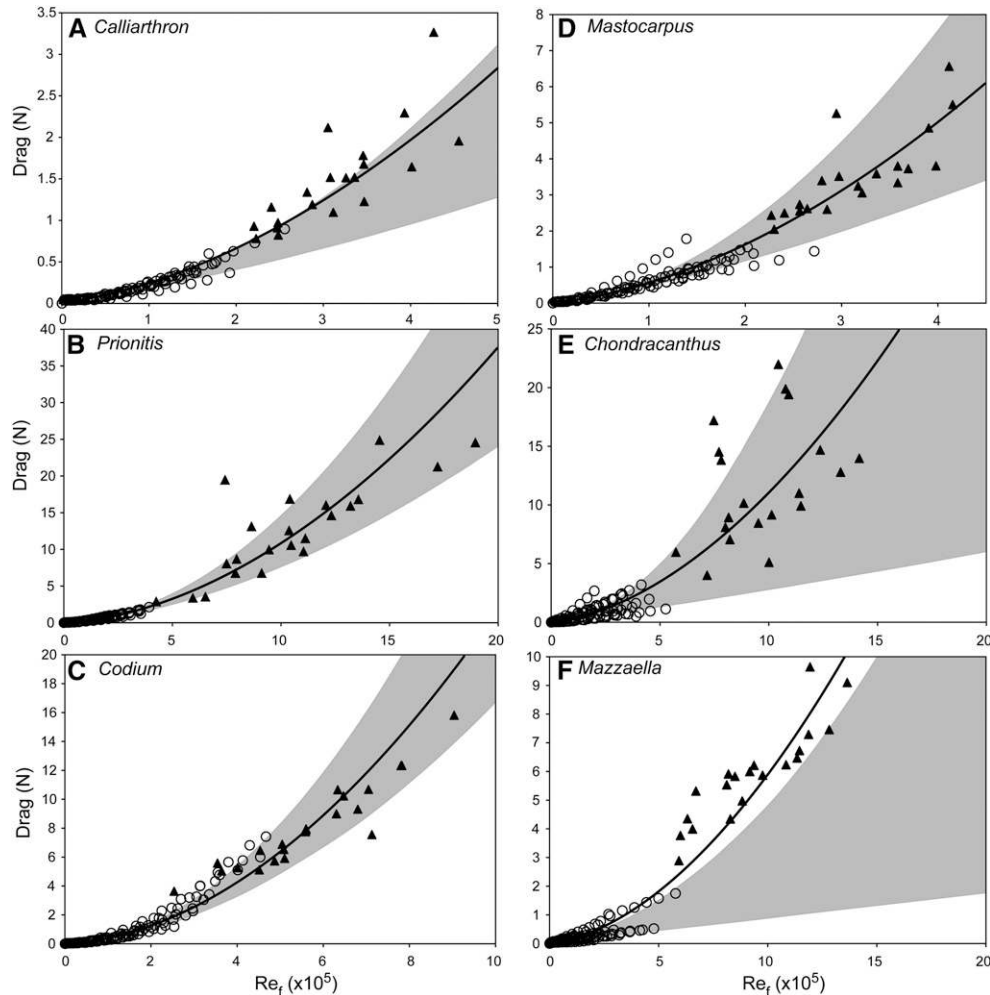


Fig. 4. Drag force ( $F_{\text{drag}}$ ) vs. frond Reynolds number ( $Re_f$ ) for each experimental species. Open circles are data collected in the recirculating flume, and gray regions represent  $\pm 95\%$  confidence intervals around predictions based on flume data alone. Black triangles are data collected in the high-speed gravity flume; solid lines are curves fitted to both recirculating and gravity flume data, as described in the methods.

modulus or flexural stiffness, to predict the ability of seaweeds to change shape or projected area in flow.

It should be noted that  $C_{d, \text{true}}$  values documented at slow-speed (Fig. 2A,  $U = 0.1 \text{ m}\cdot\text{s}^{-1}$ ) were notably high for some seaweeds, such as *Calliarthron* and *Mastocarpus*—up to 10 times greater than those reported for various engineering shapes (Vogel, 1994), which rarely exceed 1 at a comparable Reynolds number ( $>10^3$ ). The cause of these high drag coefficients is unknown and deserves further study. It may be a consequence of shear drag on irregularly shaped fronds at slow speeds or the result of fronds flapping to form unexpectedly large wakes in flow (Hoerner, 1965; Koehl and Alberte, 1988).

**Predicting drag at high velocities**—Past studies have had difficulty linking drag measured in slow-speed laboratory conditions to observed patterns of survivorship in the field. Blame is often focused on the notoriously inaccurate process of drag extrapolation. Indeed, in the current study, data collected on seaweeds in the recirculating flume did not always accurately predict drag at higher speeds. Predicted and observed drag forces at higher speeds were similar for only some of the seaweeds studied here (*Prionitis*, *Codium*, *Mastocarpus*, and

*Chondracanthus*), suggesting that measurements at slower speeds might be sufficient to predict performance of these seaweeds in the field. However, for the other seaweeds studied here (*Mazzaella* and *Calliarthron*), drag predictions underestimated actual drag measurements at high speeds, suggesting that slow-speed data collected on these seaweeds in the laboratory are misleading and are not representative of their performance in the field. That 33% of drag extrapolations were inaccurate supports and highlights the uncertainty noted in previous studies and underscores the need for researchers to think twice before drawing conclusions based on extrapolations.

The discrepancy between predicted and observed drag forces at high speeds suggests that, at least for some seaweeds, slow-speed reconfiguration in recirculating flumes may differ from high-speed reconfiguration under breaking waves. In recirculating flow, seaweeds have more time to reconfigure, bending and collapsing their branches to a greater extent as flow steadily increases; whereas, under breaking waves (and in the high-speed flume here), seaweeds are suddenly struck by incoming waves, making them susceptible to wave-impingement forces (Gaylord et al., 2008) and allowing only minimal time to reconfigure and limit drag. This difference in time-dependent

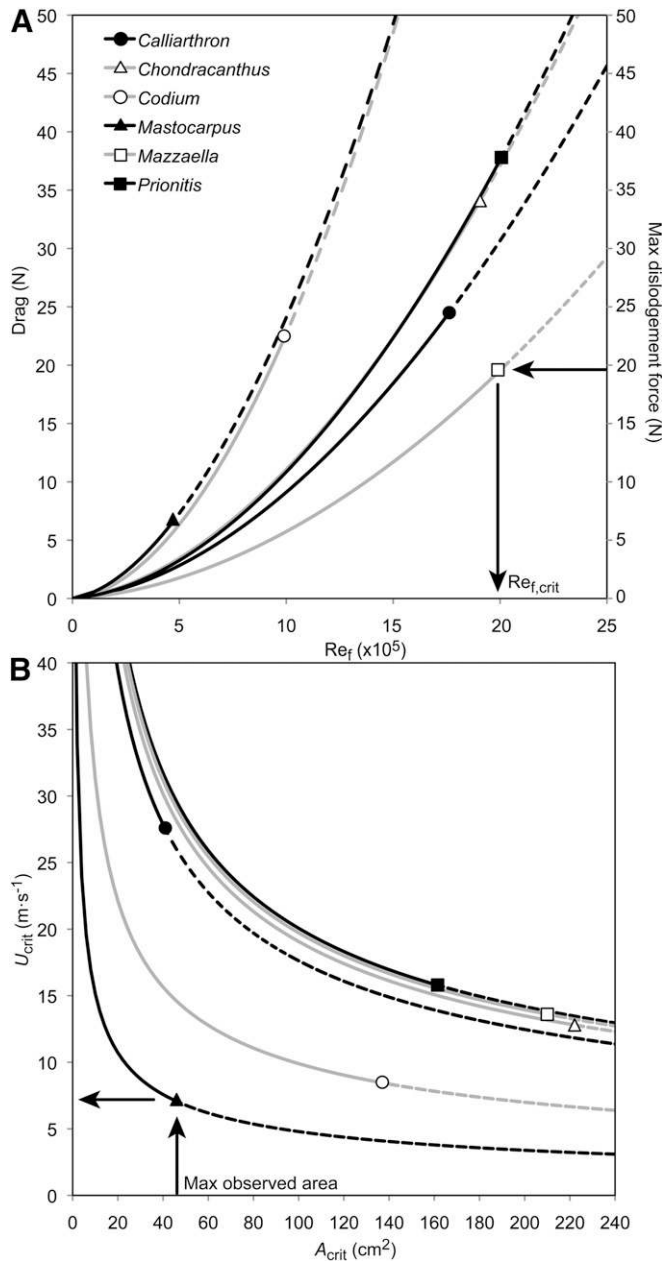


Fig. 5. Drag, maximum size, and critical water velocity predictions for seaweed thalli in the field. (A) Drag force ( $F_{drag}$ ) predictions vs. frond Reynolds number ( $Re_f$ ). Shapes represent maximum dislodgement forces, used to calculate critical  $Re_f$ . Dotted lines represent hypothetical dislodgement forces greater than the strongest alga observed. (B) Critical  $Re_f$  isoclines for each species. Shapes represent maximum frond sizes ( $A_{crit}$ ) observed in the field, used to predict the maximum water velocity ( $U_{crit}$ ) experienced by each species along the shore. Dotted lines represent hypothetical planform areas greater than the largest alga observed.

reconfiguration would explain why drag forces at higher speeds were greater than those predicted by slow-speed data (e.g., see Fig. 4F). Unfortunately, turbulent and aerated flow conditions make it impossible to photograph seaweed reconfiguration under breaking waves, preventing a complete analysis of shape change and area change at high speeds. Thus, we do not know if extrapolation error is due to

TABLE 2. Maximum observed frond sizes, dislodgement forces, and critical frond Reynolds numbers ( $Re_{f,crit}$ ) for each species.

Species	Max observed planform area (cm <sup>2</sup> )	Dislodgement force (N)			$Re_{f,crit}$ (× 10 <sup>6</sup> )
		Mean ± SD	Max	Max percentile	
<i>Calliarthron</i>	41.0	18.5 ± 5.1	24.5	89.4	1.762
<i>Codium</i>	137.0	17.1 ± 4.6	22.5	89.4	0.989
<i>Mastocarpus</i>	46.0	3.4 ± 1.4	6.6	98.7	0.479
<i>Prionitis</i>	161.5	19.1 ± 7.3	37.8	99.4	2.006
<i>Chondracanthus</i>	222.1	20.9 ± 6.3	34.1	98.4	1.907
<i>Mazzaella</i>	210.0	12.1 ± 4.1	19.6	96.7	1.972

time-dependent reconfiguration or some other hydrodynamic phenomenon.

**Predicting dislodgement**—New drag predictions based on both slow- and high-speed data show that seaweed species group together in surprising ways. As velocity and size increase (i.e.,  $Re_f$  increases), drag is predicted to increase similarly and most rapidly for thalli of *Codium* and *Mastocarpus*, two seaweeds of widely divergent branching structure and thallus construction (Fig. 5A). Perhaps more perplexing is that drag is predicted to increase similarly on branched thalli of *Prionitis* and bladed thalli of *Chondracanthus*. These data suggest that comparisons of drag experienced by bladed and branched algae may not be generalizable.

In the field, drag forces are resisted by dislodgement forces, which differ among seaweed species. Although maximum dislodgement forces varied widely among experimental seaweeds, many of these values point to strikingly similar  $Re_{f,crit}$  values that would lead to breakage. Wave-exposed thalli of *Prionitis*, *Calliarthron*, *Chondracanthus*, and *Mazzaella* are all predicted to fail when  $Re_{f,crit}$  approaches  $2 \times 10^6$ . This suggests that attachment strength and drag force may scale similarly in these wave-exposed taxa. For example, *Mazzaella* experiences relatively low drag but also has a low maximum attachment strength; *Prionitis* experiences more drag, but is stronger. Drag-related scaling patterns such as these are likely to exist in nature, since drag resistance depends critically upon the mechanical properties (e.g., strength) of supporting seaweed tissues (see Martone, 2007). The identification of common  $Re_{f,crit}$  values among morphologically distinct wave-swept taxa is interesting and deserves further study. Is there something special about this combination of velocity and frond size?

Because  $Re_{f,crit}$  values were comparable among *Prionitis*, *Calliarthron*, *Chondracanthus*, and *Mazzaella*, fronds of a given size were all predicted to resist similar water velocities. As fronds grow, slower water velocities are required to dislodge them. Therefore, the isoclines depicted in Fig. 5B can be used in combination with maximum observed frond sizes to explore the hydrodynamic environment where experimental seaweeds were collected. For example, the largest thalli collected in this study were blades of *Mazzaella* and *Chondracanthus*.  $Re_{f,crit}$  isoclines suggest that these large fronds could not have experienced water velocities greater than  $15 \text{ m}\cdot\text{s}^{-1}$ , setting an upper bound to the likely wave exposure at that intertidal site. On the other hand, the maximum size of *Calliarthron* fronds was much smaller, suggesting that intertidal *Calliarthron* fronds may have experienced up to  $28 \text{ m}\cdot\text{s}^{-1}$ . These estimates are in general agreement with past measurements of intertidal water velocities (Denny et al., 1989, 2003; Denny, 1994; Gaylord et al., 1994;

Denny and Gaylord, 2002; Martone and Denny, 2008; Mach et al., 2011). However, fronds that exceed the maximum sizes observed in this study may be found growing in the subtidal zone or in areas of reduced wave exposure.

In general, smaller fronds are not as limited by water velocities, and so it is possible that young or small mature fronds may be found growing at more wave-battered locations. Our model lacks consideration of the relationship between size and attachment strength; if small plants have lower attachment strength (e.g., Gaylord et al., 1994), then the water velocity predicted to break small fronds in Fig. 5B may be an overestimate. On the other hand, some red algae exhibit little variation in attachment strength across size classes (Carrington, 1990; Shaughnessy et al., 1996; Kitzes and Denny, 2005; Martone, 2006, 2007), so the current model may be reasonable.

The  $Re_{f, crit}$  isoclines presented here can be used to make broad comparisons across seaweed species and habitats. For a given size, fronds of *Codium* and *Mastocarpus* are predicted to break at lower water velocities than fronds produced by the other four species. This suggests that these two species may persist at wave-exposed locations, but only if they remain relatively small. The maximum observed sizes of *Mastocarpus* and *Calliarthron* were similar, but at this size, *Mastocarpus* could only resist one-quarter the critical water velocity of *Calliarthron* before being dislodged. Why the discrepancy? Perhaps *Mastocarpus* fronds living higher in the intertidal zone do not experience the same rapid water velocities experienced by *Calliarthron* and other wave-exposed algae growing in the low intertidal zone. Another possibility is that *Mastocarpus* fronds growing in tight clusters resist faster water velocities by achieving a “drafting” benefit from neighboring fronds and thereby experience less drag (Johnson, 2001; Boller and Carrington, 2006a). Similarly, the maximum size of *Codium* fronds was almost as large as other wave-swept algae, but such large fronds were predicted to break at less than  $10 \text{ m}\cdot\text{s}^{-1}$  water velocity. Large *Codium* fronds are commonly found in sheltered marinas where water velocities are slow, but fronds collected for this study were collected from a generally wave-exposed shore. Perhaps these wave-exposed *Codium* fronds survived by experiencing locally reduced flow conditions in tidepools or in the lee of big rocks. Understanding the hydrodynamic limits of intertidal seaweeds may provide an additional index of wave exposure and thereby improve predictions of local water velocities along wave-swept shores (Helmuth and Denny, 2003).

In summary, intertidal seaweeds limit wave-induced drag forces by changing shape (i.e., reducing drag coefficient) and by reducing area projected in flow. These two drag-limiting processes are intertwined but distinct and likely play a role in the morphological evolution of wave-swept seaweeds. Flexible reconfiguration permits certain bladed and branched algae to perform similarly in flow, despite morphological differences, and often complicates our ability to predict drag and dislodgement of seaweeds in the field.

#### LITERATURE CITED

- BELL, E. C. 1999. Applying flow tank measurements to the surf zone: Predicting dislodgment of the Gigartinales. *Phycological Research* 47: 159–166.
- BLANCHETTE, C. A. 1996. Seasonal patterns of disturbance influence recruitment of the sea palm, *Postelsia palmaeformis*. *Journal of Experimental Marine Biology and Ecology* 197: 1–14.
- BOLLER, M. L., AND E. CARRINGTON. 2006a. *In situ* measurements of hydrodynamic forces imposed on *Chondrus crispus* Stackhouse. *Journal of Experimental Marine Biology and Ecology* 337: 159–170.
- BOLLER, M. L., AND E. CARRINGTON. 2006b. The hydrodynamic effects of shape and size change during reconfiguration of a flexible macroalga. *Journal of Experimental Biology* 209: 1894–1903.
- BOLLER, M. L., AND E. CARRINGTON. 2007. Interspecific comparison of hydrodynamic performance and structural properties among intertidal macroalgae. *Journal of Experimental Biology* 210: 1874–1884.
- BUTLER, D. W., S. M. GLEASON, I. DAVIDSON, Y. ONODA, AND M. WESTOBY. 2012. Safety and streamlining of woody shoots in wind: An empirical study across 39 species in tropical Australia. *New Phytologist* 193: 137–149.
- CARRINGTON, E. 1990. Drag and dislodgement of an intertidal macroalga: Consequences of morphological variation in *Mastocarpus papillatus* Kützinger. *Journal of Experimental Marine Biology and Ecology* 139: 185–200.
- CONNELL, J. H. 1972. Community interactions on marine rocky intertidal shores. *Annual Review of Ecology and Systematics* 3: 169–192.
- DAYTON, P. K. 1975. Experimental evaluation of ecological dominance in a rocky intertidal algal community. *Ecological Monographs* 45: 137–159.
- DEMES, K., E. CARRINGTON, J. M. GOSLINE, AND P. T. MARTONE. 2011. Variation in anatomical and material properties explains differences in hydrodynamic performance of foliose red macroalgae. *Journal of Phycology*.
- DENNY, M. W. 1988. *Biology and mechanics of the wave-swept environment*. Princeton University Press, Princeton, New Jersey, USA.
- DENNY, M. W. 1994. Extreme drag forces and the survival of wind- and water-swept organisms. *Journal of Experimental Biology* 194: 97–115.
- DENNY, M. W., V. BROWN, E. CARRINGTON, G. P. KRAEMER, AND A. MILLER. 1989. Fracture mechanics and the survival of wave-swept macroalgae. *Journal of Experimental Marine Biology and Ecology* 127: 211–228.
- DENNY, M. W., AND B. GAYLORD. 2002. The mechanics of wave-swept algae. *Journal of Experimental Biology* 205: 1355–1362.
- DENNY, M. W., B. P. GAYLORD, AND E. A. COWEN. 1997. Flow and flexibility II. The roles of size and shape in determining wave forces on the bull kelp *Nereocystis luetkeana*. *Journal of Experimental Biology* 200: 3165–3183.
- DENNY, M. W., L. P. MILLER, M. D. STOKES, L. J. H. HUNT, AND B. S. T. HELMUTH. 2003. Extreme water velocities: Topographical amplification of wave-induced flow in the surf zone of rocky shores. *Limnology and Oceanography* 48: 1–8.
- DENNY, M. W., AND D. WETHEY. 2001. Physical processes that generate patterns in marine communities. In M. D. Bertness, S. Gaines, and M. E. Hay [eds.], *Marine community ecology*, 3–37. Sinauer, Sunderland, Massachusetts, USA.
- ERON, B., AND R. J. TIBSHIRANI. 1993. *An introduction to the bootstrap*. Chapman & Hall/CRC, New York, New York, USA.
- ENNOS, A. R. 1997. Wind as an ecological factor. *Trends in Ecology & Evolution* 12: 108–111.
- ENNOS, A. R. 1999. The aerodynamics and hydrodynamics of plants. *Journal of Experimental Biology* 202: 3281–3284.
- GAYLORD, B. 2000. Biological implications of surf-zone flow complexity. *Limnology and Oceanography* 45: 174–188.
- GAYLORD, B., C. A. BLANCHETTE, AND M. W. DENNY. 1994. Mechanical consequences of size in wave-swept algae. *Ecological Monographs* 64: 287–313.
- GAYLORD, B., AND M. W. DENNY. 1997. Flow and flexibility I. Effects of size, shape and stiffness in determining wave forces on the stipitate kelps *Eisenia arborea* and *Pterygophora californica*. *Journal of Experimental Biology* 200: 3141–3164.
- GAYLORD, B., M. W. DENNY, AND M. A. R. KOEHL. 2008. Flow forces on seaweeds: Field evidence for roles of wave impingement and organism inertia. *Biological Bulletin* 215: 295–308.
- HARDER, D., O. SPECK, C. HURD, AND T. SPECK. 2004. Reconfiguration as a prerequisite for survival in highly unstable flow-dominated environments. *Journal of Plant Growth Regulation* 23: 98–107.



- HARLEY, C. D. G. 2003. Abiotic stress and herbivory interact to set range limits across a two-dimensional stress gradient. *Ecology* 84: 1477–1488.
- HARLEY, C. D. G., AND B. S. T. HELMUTH. 2003. Local- and regional-scale effects of wave exposure, thermal stress, and absolute versus effective shore level on patterns of intertidal zonation. *Limnology and Oceanography* 48: 1498–1508.
- HARLEY, C. D. G., AND R. T. PAINE. 2009. Contingencies and compounded rare perturbations dictate sudden distributional shifts during periods of gradual climate change. *Proceedings of the National Academy of Sciences, USA* 106: 11172–11176.
- HELMUTH, B., AND M. W. DENNY. 2003. Predicting wave exposure in the rocky intertidal zone: Do bigger waves always lead to larger forces? *Limnology and Oceanography* 48: 1338–1345.
- HOERNER, S. F. 1965. Fluid-dynamic drag: Practical information on aerodynamic and hydrodynamic resistance. S.F. Hoerner, Midland Park, New Jersey, USA.
- HURD, C. 2000. Water motion, marine macroalgal physiology, and production. *Journal of Phycology* 36: 453–472.
- JOHNSON, A. S. 2001. Drag, drafting, and mechanical interactions in canopies of the red alga *Chondrus crispus*. *Biological Bulletin* 201: 126–135.
- KITZES, J. A., AND M. W. DENNY. 2005. Red algae respond to waves: Morphological and mechanical variation in *Mastocarpus papillatus* along a gradient of force. *Biological Bulletin* 208: 114–119.
- KOEHL, M. A. R. 1986. Seaweeds in moving water: Form and mechanical function. In T. J. Givnish [ed.], *On the economy of plant form and function*, 603–634. Cambridge University Press, London, UK.
- KOEHL, M. A. R. 2000. Mechanical design and hydrodynamics of blade-like algae: *Chondracanthus exasperatus*. In H. C. Spatz and T. Speck [eds.], *Third International Plant Biomechanics Conference*. Thieme Verlag, Stuttgart, Germany.
- KOEHL, M. A. R., AND R. S. ALBERTE. 1988. Flow, flapping, and photosynthesis of *Nereocystis luetkeana*: A functional comparison of undulate and flat blade morphologies. *Marine Biology* 99: 435–444.
- LEWIS, J. R. 1968. Water movements and their role in rocky shore ecology. *Sarsia* 34: 13–36.
- MACH, K. J. 2009. Mechanical and biological consequences of repetitive loading: Crack initiation and fatigue failure in the red macroalga *Mazzaella*. *Journal of Experimental Biology* 212: 961–976.
- MACH, K. J., D. V. NELSON, AND M. W. DENNY. 2007. Techniques for predicting the lifetimes of wave-swept macroalgae: A primer on fracture mechanics and crack growth. *Journal of Experimental Biology* 210: 2213–2230.
- MACH, K. J., S. K. TEPLER, A. V. STAAR, J. C. BOHNHOFF, AND W. DENNY. 2011. Failure by fatigue in the field: A model of fatigue breakage for the macroalga *Mazzaella*, with validation. *Journal of Experimental Biology* 214: 1571–1585.
- MARTONE, P. T. 2006. Size, strength and allometry of joints in the articulated coralline *Calliarthron*. *Journal of Experimental Biology* 209: 1678–1689.
- MARTONE, P. T. 2007. Kelp versus coralline: Cellular basis for mechanical strength in the wave-swept seaweed *Calliarthron* (Corallinaceae, Rhodophyta). *Journal of Phycology* 43: 882–891.
- MARTONE, P. T., AND M. W. DENNY. 2008. To break a coralline: Mechanical constraints on the size and survival of a wave-swept seaweed. *Journal of Experimental Biology* 211: 3433–3441.
- NIKLAS, K. J., AND T. SPECK. 2001. Evolutionary trends in safety factors against wind-induced stem failure. *American Journal of Botany* 88: 1266–1278.
- PAINE, R. T. 1979. Disaster, catastrophe, and local persistence of the sea palm *Postelsia palmaeformis*. *Science* 205: 685–687.
- PAINE, R. T., AND S. A. LEVIN. 1981. Intertidal landscapes: Disturbance and the dynamics of pattern. *Ecological Monographs* 51: 145–178.
- SHAUGHNESSY, F. J., R. E. DEWREEDE, AND E. C. BELL. 1996. Consequences of morphology and tissue strength to blade survivorship of two closely related Rhodophyta species. *Marine Ecology Progress Series* 136: 257–266.
- SOKAL, R. R., AND F. J. ROHLF. 2001. *Biometry: The principles and practice of statistics in biological research*, 3rd ed. W. H. Freeman, New York, New York, USA.
- SOUSA, W. P. 1979. Experimental investigations of disturbance and ecological succession in a rocky intertidal algal community. *Ecological Monographs* 49: 227–254.
- STACHOWICZ, J. J., M. GRAHAM, M. E. S. BRACKEN, AND A. I. SZOBOSZLAI. 2008. Diversity enhances cover and stability of seaweed assemblages: The role of heterogeneity and time. *Ecology* 89: 3008–3019.
- VOGEL, S. 1989. Drag and reconfiguration of broad leaves in high winds. *Journal of Experimental Botany* 40: 941–948.
- VOGEL, S. 1994. *Life in moving fluids*, 2nd ed. Princeton University Press, Princeton, New Jersey, USA.